Do Image Classifiers Generalize Across Time?

Vaishaal Shankar*
UC Berkeley

Achal Dave*
CMU

Rebecca Roelofs
UC Berkeley

Deva Ramanan
CMU

Benjamin Recht
UC Berkeley

Ludwig Schmidt
UC Berkeley

Abstract

We study the robustness of image classifiers to temporal perturbations derived from videos. As part of this study, we construct two datasets [1], `ImageNet-Vid-Robust` and `YTBB-Robust`, containing a total of 57,897 images grouped into 3,139 sets of perceptually similar images. Our datasets were derived from ImageNet-Vid and Youtube-BB respectively and thoroughly re-annotated by human experts for image similarity. We evaluate a diverse array of classifiers pre-trained on ImageNet and show a median classification accuracy drop of 16 and 10 on our two datasets. Additionally, we evaluate three detection models and show that natural perturbations induce both classification as well as localization errors, leading to a median drop in detection mAP of 14 points. Our analysis demonstrates that perturbations occurring naturally in videos pose a substantial and realistic challenge to deploying convolutional neural networks in environments that require both reliable and low-latency predictions.

1   Introduction

Convolutional neural networks (CNNs) still exhibit many troubling failure modes. At one extreme, ℓ_p-adversarial examples cause large drops in accuracy for state-of-the-art models while relying only on visually imperceptible changes to the input image [3, 11]. However, this failure mode usually does not pose a problem outside a fully adversarial context because carefully crafted ℓ_p-perturbations are unlikely to occur naturally in the real world.

To study more realistic failure modes, researchers have investigated benign image perturbations such as rotations & translations, colorspace changes, and various image corruptions [6, 7, 14, 15]. However, it is still unclear whether these perturbations reflect the robustness challenges arising in real data since the perturbations also rely on synthetic image modifications.

Recent work has therefore turned to videos as a source of *naturally occurring* perturbations of images [1, 12, 31]. In contrast to other failure modes, the perturbed images are taken from existing image

---

*Equal contribution
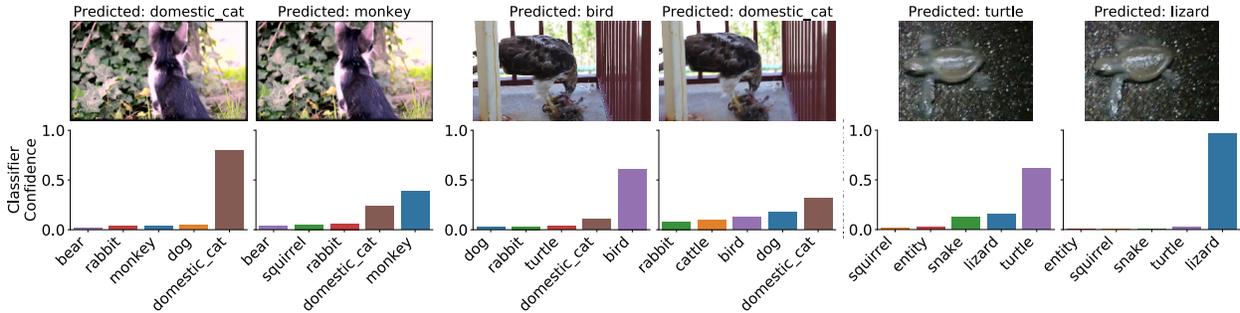[1]Our datasets are available at this url: https://modestyachts.github.io/robust-vid/

Figure 1: Three examples of natural perturbations from nearby video frames and resulting classifier predictions from a ResNet-152 model fine-tuned on ImageNet-Vid. While the images appear almost identical to the human eye, the classifier confidence changes substantially.

data without further modifications to make the task more difficult. As a result, robustness to such perturbations directly corresponds to performance improvements on real data.

However, it is currently unclear to what extent such video perturbations pose a robustness challenge. Azulay and Weiss [1] and Zheng et al. [31] only provide anecdotal evidence from a small number of videos. Gu et al. [12] go beyond individual videos and utilize a large video dataset [24] in order to measure the effect of video perturbations more quantitatively. In their evaluation, the best image classifiers lose about 3% accuracy for video frames up to 0.3 seconds away. However, the authors did not employ humans to review the frames in their videos. Hence the accuracy drop could also be caused by significant changes in the video frames (e.g., due to fast camera or object motion). Since the 3% accuracy drop is small to begin with, it remains unclear whether video perturbations are a robustness challenge for current image classifiers.

We address these issues by conducting a thorough evaluation of robustness to natural perturbations arising in videos. As a cornerstone of our investigation, we introduce two test sets for evaluating model robustness: `ImageNet-Vid-Robust` and `YTBB-Robust`, carefully curated from the ImageNet-Vid and Youtube-BB datasets, respectively [24, 27]. All images in the two datasets were screened by a set of expert labelers to ensure high annotation quality and minimize selection biases that arise when filtering a dataset with CNNs. To the best of our knowledge these are the first datasets of their kind, containing tens of thousands of images that are *human reviewed* and grouped into thousands of perceptually similar sets. In total, our datasets contain 3,139 sets of temporally adjacent and visually similar images (57,897 images total).

We then utilize these datasets to measure the robustness of current CNNs to small, naturally occurring perturbations. Our testbed contains over 45 different models, varying both architecture and training methodology (adversarial training, data augmentation, etc.). To better understand the drop in accuracy due to natural perturbations, we also introduce a robustness metric that is more stringent than those employed in prior work. Under this metric, we find that natural perturbations from `ImageNet-Vid-Robust` and `YTBB-Robust` induce a median accuracy drop of 16% and 10% respectively for classification tasks and a median 14 point drop in mAP for detection tasks.[2] Even for the best-performing classification models, we observe an accuracy drop of 14% for

---

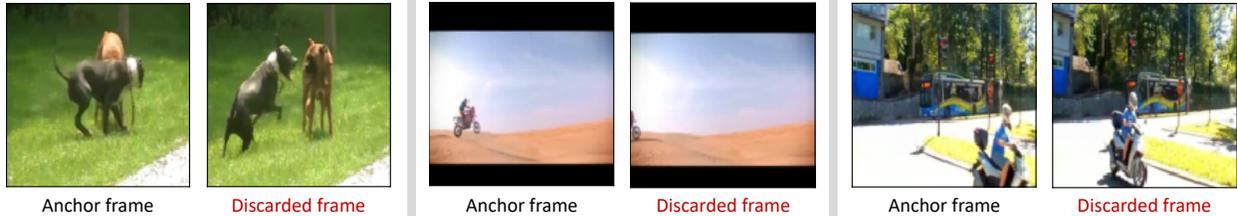[2]We only evaluated detection on `ImageNet-Vid-Robust` as bounding-box annotations in Youtube-BB are

Figure 2: Temporally adjacent frames may not be visually similar. We show three randomly sampled frame pairs where the nearby frame was marked as "dissimilar" to the anchor frame during human review and then discarded from our dataset.

`ImageNet-Vid-Robust` and 8% for `YTBB-Robust`.

Our results show that robustness to natural perturbations in videos is indeed a significant challenge for current CNNs. As these models are increasingly deployed in safety-critical environments that require both high accuracy and low latency (e.g., autonomous vehicles), ensuring reliable predictions on *every frame* of a video is an important direction for future work.

2 Constructing a test set for robustness

`ImageNet-Vid-Robust` and `YTBB-Robust` are sourced from videos in the ImageNet-Vid and Youtube-BB datasets [24, 27]. All object classes in ImageNet-Vid and Youtube-BB are from the WordNet hierarchy [22] and direct ancestors of ILSVRC-2012 classes. Using the WordNet hierarchy, we construct a canonical mapping from ILSVRC-2012 classes to ImageNet-Vid and Youtube-BB classes, which allows us to evaluate off-the-shelf ILSVRC-2012 models on `ImageNet-Vid-Robust` and `YTBB-Robust`. We provide more background on the source datsets in Appendix A.

2.1 Constructing **ImageNet-Vid-Robust** and **YTBB-Robust**

Next, we describe how we extracted sets of naturally perturbed frames from ImageNet-Vid and Youtube-BB to create `ImageNet-Vid-Robust` and `YTBB-Robust`. A straightforward approach would be to select a set of anchor frames and use temporally adjacent frames in the video with the assumption that such frames contain only small perturbations from the anchor. However, as Figure 2 illustrates, this assumption is frequently violated, especially due to fast camera or object motion.

Instead, we first collect *preliminary* datasets of natural perturbations following the same approach, and then manually review each of the frame sets. For each video, we randomly sample an anchor frame and take $k = 10$ frames before and after the anchor frame as candidate perturbation images.[3] This results in two datasets containing one anchor frame each from 3,139 videos, with approximately 20 candidate perturbation per anchor frame.[4]

---

available only at a temporal resolution of 1 frame-per-second and hence not dense enough for our evaluation.

[3] For `YTBB-Robust` we use a subset of the anchor frames used by Gu et al. [12].

[4] Anchor frames near the start or end of the video may have less than 20 candidate frames.

		ImageNet-Vid-Robust	YTBB-Robust
	Reviewed	1,314	2,467
Anchor frames	Accepted	1,109 (84%)	2,030 (82%)
	Labels updated	-	834 (41%)
Frame pairs	Reviewed	26,029	45,631
	Accepted	21,070 (81%)	36,827 (81%)

Table 1: Dataset statistics of `ImageNet-Vid-Robust` and `YTBB-Robust`. For `YTBB-Robust`, we updated the labels from for 41% (834) of the accepted anchors due to incomplete labels in Youtube-BB.

Next, we curate the dataset with the help of four expert human annotators. The goal of the curation step is to ensure that each anchor frame and its nearby frames are correctly labeled with the same ground truth class, and that the anchor frame and the nearby frames are visually similar.

Denser labels for Youtube-BB. As Youtube-BB contains only a single category label per frame at 1 frame per second, annotators first inspected each anchor frame individually and added any missing labels. In total, annotators corrected the labels for 834 frames, adding an average of 0.5 labels per anchor frame. These labels are then propagated to nearby, unlabeled frames at the native frame rate and verified in the next step. ImageNet-Vid densely labels all classes per frame, so we skipped this step for this dataset.

Frame pairs review. Next, for each pair of anchor and nearby frames, a human annotates (i) whether the pair is correctly labeled in the dataset, and (ii) whether the pair is similar. We took several steps to mitigate the subjectivity of this task and ensure high annotation quality. First, we trained reviewers to mark frames as dissimilar if the scene undergoes any of the following transformations: significant motion, significant background change, or significant blur change. We asked reviewers to mark each dissimilar frame with one of these transformations, or "other", and to mark a pair of images as dissimilar if a distinctive feature of the object is only visible in one of the two frames (such as the face of a dog). If an annotator was unsure about the correct label, she could mark the pair as "unsure". Second, we present only a single pair of frames at a time to reviewers because presenting videos or groups of frames could cause them to miss large changes due to the phenomenon of change blindness [23].

Verification. In the previous stage, all annotators were given identical labeling instructions and individually reviewed a total of 71,660 image pairs. To increase consistency in annotation, annotators jointly reviewed all frames marked as dissimilar, incorrectly labeled, or "unsure". A frame was only considered similar to its anchor if a strict majority of the annotators marked the pair as such.

After the reviewing was complete, we discarded all anchor frames and candidate perturbations that annotators marked as dissimilar or incorrectly labeled. The final datasets contain a combined total of 3,139 anchor frames with a median of 20 similar frames each.

2.2 The `pm-k` evaluation metric

Given the datasets introduced above, we propose a metric to measure a model's robustness to natural perturbations. In particular, let $A = \{a_1, ..., a_n\}$ be the set of valid anchor frames in our dataset. Let $Y = \{y_1, ..., y_n\}$ be the set of labels for A. We let $\mathcal{N}_k(a_i)$ be the set of frames marked as similar to anchor frame a_i. In our setting, $\mathcal{N}_k$ is a subset of the $2k$ temporally adjacent frames (plus/minus k frames from the anchor).

Classification. The standard classification accuracy on the anchor frame is $\mathrm{acc_{orig}} = 1 - \frac{1}{N} \sum_{i=1}^{N} \mathcal{L}_{0/1}(f(a_i), y_i)$, where $\mathcal{L}_{0/1}$ is the standard 0-1 loss function. We define the `pm-k` analog of accuracy as

$$\mathrm{acc_{pmk}} = 1 - \frac{1}{N} \sum_{i=1}^{N} \max_{b \in \mathcal{N}_k(a_i)} \mathcal{L}_{0/1}(f(b), y_i) , \tag{1}$$

which corresponds to picking the worst frame from each set $\mathcal{N}_k(a_i)$ before computing accuracy. We note the similarity of the `pm-k` metric to standard ℓ_p adversarial robustness. If we let $\mathcal{N}_k(a_i)$ be the set of *all* images within an ℓ_p ball of radius ϵ around a_i, then the two notions of robustness are identical.

Detection. The standard metric for detection is mean average precision (mAP) of the predictions at a fixed intersection-over-union (IoU) threshold [20]. We define the `pm-k` metric analogous to that for classification: We replace each anchor frame with the nearest frame that minimizes the average precision (AP, averaged over recall thresholds) of the predictions, and compute `pm-k` as the mAP on these worst-case neighboring frames.

3 Main results

We evaluate a testbed of 45 classification and three detection models on `ImageNet-Vid-Robust` and `YTBB-Robust`. We first discuss the various types of classification models evaluated with the `pm-k` classification metric. Second, we evaluate the performance of detection models on `ImageNet-Vid-Robust` using use the bounding box annotations inherited from ImageNet-Vid and using a variant of the `pm-k` metric for detection. We then analyze the errors made on the detection adversarial examples to isolate the effects of *localization* errors vs. *classification* errors.

3.1 Classification

The classification robustness metric is $\mathrm{acc_{pmk}}$ defined in Equation (1). For frames with multiple labels, we count a prediction as correct if the model predicts *any* of the correct classes for a frame. In Figure 3, we plot the benign accuracy, $\mathrm{acc_{orig}}$, versus the robust accuracy, $\mathrm{acc_{pmk}}$, for all classification models in our test bed and find that the relationship between $\mathrm{acc_{orig}}$ and $\mathrm{acc_{pmk}}$ is approximately linear. This relationship indicates that improvements in the benign accuracy do

result in improvements in the worst-case accuracy, but do not suffice to resolve the accuracy drop due to natural perturbations.

Our test bed consists of five model types with increasing levels of supervision. We present results for representative models from each model type in Table 2 and defer the full classification results table to Appendix B.

ILSVRC Trained   The WordNet hierarchy enables us to repurpose models trained for the 1,000 class ILSVRC-2012 dataset on `ImageNet-Vid-Robust` and `YTBB-Robust` (see Appendix A.1). We evaluate a wide array of ILSVRC-2012 models (available from [4]) against our natural perturbations. Since these datasets present a substantial distribution shift from the original ILSVRC-2012 validation set, we expect the *benign* accuracy $\mathrm{acc_{orig}}$ to be lower than the comparable accuracy on the ILSVRC-2012 validation set. However, our main interest here is in the *difference* between the original and perturbed accuracies $\mathrm{acc_{orig}}$ - $\mathrm{acc_{pmk}}$. A small drop in accuracy would indicate that the model is robust to small changes that occur naturally in videos. Instead, we find significant median drops of 15.0% and 13.2% in accuracy on our two datasets, indicating sensitivity to such changes.

Noise augmentation   One hypothesis for the accuracy drop from original to perturbed accuracy is that subtle artifacts and corruptions introduced by video compression schemes could degrade performance when evaluating on these corrupted frames. The worst-case nature of the `pm-k` metric could then be focusing on these corrupted frames. One model for these corruptions are the perturbations introduced in [14]. To test this hypothesis, we evaluate models augmented with a subset of the perturbations (exactly one of: Gaussian noise, Gaussian blur, shot noise, contrast change, impulse noise, or JPEG compression). We found that these augmentation schemes did not improve robustness against our perturbations substantially, and still result in a median accuracy drop of 15.6% and 16.6% on the two datasets.
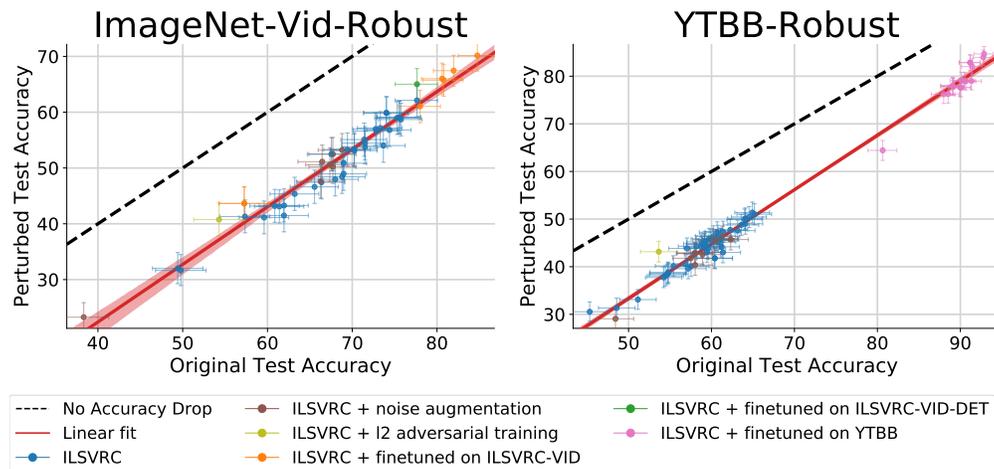

Figure 3: Model accuracy on original vs. perturbed images. Each data point corresponds to one model in our testbed (shown with 95% Clopper-Pearson confidence intervals). Each perturbed frame was taken from a ten frame neighborhood of the original frame (approximately 0.3 seconds). All frames were reviewed by humans to confirm visual similarity to the original frames.

Table 2: Accuracies of five different model types and the best performing model (shown with 95% Clopper-Pearson confidence intervals). Δ denotes accuracy drop between evaluation on anchor frame (`pm-0`) and worst frame in similarity set (`pm-10`). The model architecture is ResNet-50 unless noted otherwise. 'FT' denotes 'fine-tuning.' See Section 3.1 for details.

Model Type	Accuracy Original	Accuracy Perturbed	Δ
`ImageNet-Vid-Robust`			
Trained on ILSVRC	67.5 [64.7, 70.3]	52.5 [49.5, 55.5]	15.0
+ Noise Augmentation	68.8 [66.0, 71.5]	53.2 [50.2, 56.2]	15.6
+ ℓ_∞ robustness (ResNext-101)	54.3 [51.3, 57.2]	40.8 [39.0, 43.7]	12.4
+ FT on ImageNet-Vid	80.8 [78.3, 83.1]	65.7 [62.9, 68.5]	15.1
+ FT on ImageNet-Vid (ResNet-152)	84.8 [82.5, 86.8]	70.2 [67.4, 72.8]	14.6
+ FT on ImageNet-Vid-Det	77.6 [75.1, 80.0]	65.4 [62.5, 68.1]	12.3
`YTBB-Robust`			
Trained on ILSVRC	57.0 [54.9, 59.2]	43.8 [41.7, 46.0]	13.2
+ Noise Augmentation	62.3 [60.2, 64.4]	45.7 [43.5, 47.9]	16.6
+ ℓ_∞ robustness (ResNext-101)	53.6 [51.4, 55.8]	43.2 [41.0, 45.3]	10.4
+ FT on Youtube-BB	91.4 [90.1, 92.6]	82.0 [80.3, 83.7]	9.4
+ FT on Youtube-BB (ResNet-152)	92.9 [91.6, 93.9]	84.7 [83.0, 86.2]	8.2

ℓ_∞-robustness. We evaluate the model from [30], which currently performs best against ℓ_∞-attacks on ImageNet. We find that this model has a smaller accuracy drop than the two aforementioned model types on both datasets. However, the robust model achieves substantially lower original and perturbed accuracy than either of the two model types above, and the robustness gain is modest (3% compared to models of similar benign accuracy).

Fine-tuning on video frames. To adapt to the new class vocabulary and the video domain, we fine-tune several network architectures on the ImageNet-Vid and Youtube-BB training sets. For Youtube-BB, we train on the anchor frames used for training in [12], and for ImageNet-Vid we use all frames in the training set. We provide hyperparameters for all models in Appendix K.

The resulting models significantly improve in accuracy over their ILSVRC pre-trained counterparts (e.g., 13% on `ImageNet-Vid-Robust` and 34% on `YTBB-Robust` for ResNet-50). This improvement in accuracy results in a modest improvement in the accuracy drop for `YTBB-Robust`, but a finetuned ResNet-50 still suffers from a substantial 9.4% drop. On `ImageNet-Vid-Robust`, there is almost no change in the accuracy drop from 15.0% to 15.1%.

Fine-tuning for detection on video frames. We further analyze whether additional supervision in the form of bounding box annotations improves robustness. To this end, we train the Faster R-CNN *detection* model [26] with a ResNet-50 backbone on ImageNet-Vid. Following standard practice, the detection backbone is pre-trained on ILSVRC-2012. To evaluate this detector for classification, we assign the class with the most confident bounding box as label to the image. We find that this transformation reduces accuracy compared to the model trained for classification (77.6% vs. 80.8%). While there is a slight reduction in the accuracy drop caused by natural perturbations,

Table 3: Detection and localization mAP for two Faster R-CNN backbones. Both detection and localization suffer from significant drops in mAP due to the perturbations. (* indicates that the model has trained on the ILSVRC Det and VID 2015 datasets and evaluated on the 2015 subset of ILSVRC-VID 2017.)

Task	Model	mAP Original	mAP Perturbed	mAP Δ
Detection	FRCNN, ResNet 50	62.8	48.8	14.0
	FRCNN, ResNet 101	63.1	50.6	12.5
	R-FCN, ResNet 101 [29]*	79.4*	63.7*	15.7*
Localization	FRCNN, ResNet 50	76.6	64.2	12.4
	FRCNN, ResNet 101	77.8	66.3	11.5
	R-FCN, ResNet 101*	80.9*	70.3*	10.6*

the reduction is well within the error bars for this test set. We leave an in-depth investigation of additional supervision to induce robustness for future work.

3.2 Detection

We further study the impact of natural perturbations on object detection. Specifically, we report results for two related tasks: object localization and detection. Object detection is the standard computer vision task of correctly classifying an object and finding the coordinates of a tight bounding box containing the object. "Object localization", meanwhile, refers to only the subtask of finding the bounding box, *without* attempting to correctly classify the object.

We provide our results on `ImageNet-Vid-Robust`, which contains dense bounding box labels unlike Youtube-BB, which only labels boxes at 1 frame per second. We use the popular Faster R-CNN [26] and R-FCN [5, 29] architectures for object detection and localization and report results in Table 3. For the R-FCN architecture, we use the model from [29][5]. We first note the significant drop in mAP of 12 to 15 points for object detection due to perturbed frames for both the Faster R-CNN and R-FCN architectures. Next, we show that localization is indeed easier than detection, as the mAP is higher for localization than for detection (e.g., 76.6 vs 62.8 for Faster R-CNN with a ResNet-50 backbone). Perhaps surprisingly, however, switching to the localization task does *not* improve the drop between original and perturbed frames, indicating that natural perturbations induce both classification and localization errors. We show examples of detection failures in Figure 4.

3.3 Impact of dataset review

We analyze the impact of our human review, described in Section 2.1, on the classifiers in our testbed. First, we compare the original and perturbed accuracies of a representative classifier (ResNet-152 finetuned) with and without review in Table 4. Our review improves the original accuracy by 3 to 4% by discarding mislabeled or blurry anchor frames, and improves perturbed accuracy by 5

---

[5]This model was originally trained on the 2015 subset of ImageNet-Vid. We evaluated this model on the 2015 validation set because the method requires access to pre-computed bounding box proposals which are available only for the 2015 subset of ImageNet-Vid.

Figure 4: Naturally perturbed examples for detection. Red boxes indicate false positives; green boxes indicate true positives; white boxes are ground truth. Classification errors are common failures, such as the fox on the left, which is classified correctly in the anchor frame, and misclassified as a sheep in a nearby frame. However, detection models also have *localization* errors, where the object of interest is not correctly localized in addition to being misclassified, such as the airplane (middle) and the motorcycle (right). All visualizations show predictions with confidence greater than 0.5.

to 6% by discarding pairs of dissimilar frames. Our review reduces the accuracy drop by 1.8% on `ImageNet-Vid-Robust` and 1.1% on `YTBB-Robust`. These results indicate that the changes in model predictions are indeed due to a lack of robustness, rather than due to significant differences between adjacent frames.

To further analyze the impact of our review on model errors, we plot how frequently each offset distance from the anchor frame results in a model error across all model types in Figure 5. For both datasets, larger offsets (indicating pairs of frames further apart in time) lead to more frequent model errors. Our review reduces the fraction of errors across offsets, especially for large offsets, which are more likely to display large changes from the anchor frame.

Table 4: Impact of human review on original and perturbed accuracies for `ImageNet-Vid-Robust` and `YTBB-Robust`, numbers come from a ResNet-152 fine-tuned on ImageNet-Vid and Youtube-BB, respectively.

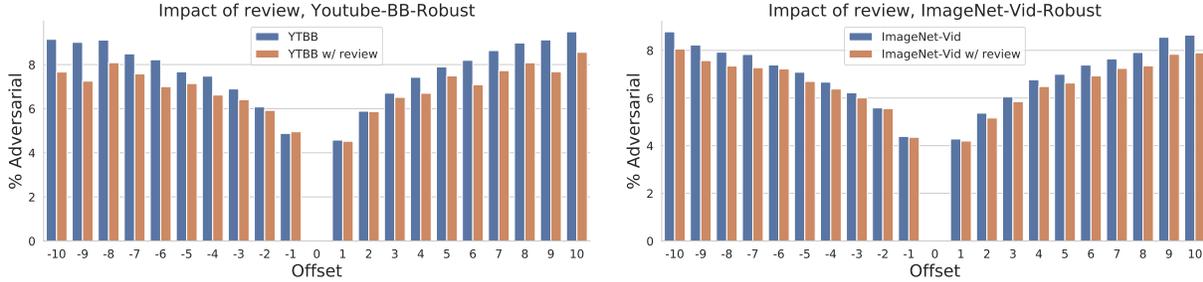|		Accuracy		
	Reviewed	Original	Perturbed	Δ
ImageNet-Vid-Robust	✗	80.3	64.1	16.2
	✓	84.8	70.2	14.4
YTBB-Robust	✗	88.1	78.1	10.0
	✓	92.9	84.7	8.9

9

Figure 5: We plot the fraction of times each offset caused an error, across all evaluated models, for frames with and without review. Frames further away more frequently cause classifiers to misfire. Our review process reduces the number of errors, especially for frames further in time, by removing dissimilar frames.

4 Related work

Adversarial examples. Various forms of adversarial examples have been studied, the majority of research focuses on ℓ_p robustness [3, 11]. However, it is unclear whether adversarial examples pose a problem for robustness outside of a truly worst case context. It is an open question whether perfect robustness against a ℓ_p adversary will induce robustness to realistic image distortions such as those studied in this paper. Recent work has proposed less adversarial image modifications such as small rotations & translations [1, 6, 7, 17], hue and color changes [15], image stylization [9] and synthetic image corruptions such as Gaussian blur and JPEG compression [10, 14]. Even though the above examples are more realistic than the ℓ_p model, they still synthetically modify the input images to generate perturbed versions. In contrast, our work performs no synthetic modification and instead uses images that naturally occur in videos.

Utilizing videos to study robustness. In work concurrent to ours, Gu et al. [12] exploit the temporal structure in videos to study robustness. However, their experiments suggest a substantially smaller drop in classification accuracy. The primary reason for this is a less stringent metric used in [12]. By contrast, our PM-k metric is inspired by the "worst-of-k" metric used in prior work [6], highlighting the sensitivity of models to natural perturbations. In Appendix E we study the differences between the two metrics in more detail. Furthermore, the lack of human review and the high label error-rate we discovered in Youtube-BB(Table 1) presents a potentially troubling confounding factor that we resolve in our work.

Distribution shift. Small, benign changes in the test distribution are often referred to as *distribution shift*. Recht et al. [25] explore this phenomenon by constructing new test sets for CIFAR-10 and ImageNet and observe substantial performance drops for a large suite of models on the newly constructed test sets. Similar to our Figure 3, the relationship between their original and new test set accuracies is also approximately linear. However, the images in their test set bear little visual similarity to images in the original test set, while all of our failure cases in `ImageNet-Vid-Robust` and `YTBB-Robust` are on perceptually similar images. In a similar vein of study, [28] studies distribution shift *across* different computer vision data sets such as Caltech-101, PASCAL, and

ImageNet.

Temporal Consistency in Computer Vision A common issue when applying image based models to videos is *flickering*, where object detectors spuriously produce false-positives or false-negatives in isolated frames or groups of frames. [16] explicitly identify such failures and use a technique reminiscent of adversarially robust training to improve image-based models. A similar line of work focuses on improving object detection in videos as objects become occluded or move quickly [8, 18, 29, 32]. The focus in this line of work has generally been on improving object detection when objects transform in a way that makes recognition difficult from a single frame, such as fast motion or occlusion. In this work, we document a broader set of failure cases for image-based classifiers and detectors and show that failures occur when the neighboring frames are imperceptibly different.

5   Conclusion

Our study quantifies the sensitivity of image classifiers to naturally occuring temporal perturbations. These perturbations cause significant drops in accuracy for a wide range of models in both classification and detection. Our work on analyzing this failure mode opens multiple avenues for future research:

Building more robust models. Our `ImageNet-Vid-Robust` and `YTBB-Robust` datasets provide a standard measure for robustness that can be used to evaluate to any classification or detection model. In Table 2, we evaluated several commonly used models and found that all of them suffer from substantial accuracy drops due to natural perturbations. In particular, we found that model improvements with respect to artificial perturbations (such as image corruptions or ℓ_∞ adversaries) induce at best modest improvements in robustness. We hope that our standardized datasets and evaluation metric will enable future work to quantify improvements in natural robustness directly.

Further natural perturbations. Videos provide a straightforward method for collecting natural perturbations of images, enabling the study of realistic forms of robustness for machine learning methods. Other methods for generating these natural perturbations are likely to provide additional insights into model robustness. As an example, photo sharing websites contain a large number of near-duplicate images: pairs of images of the same scene captured at different times, viewpoints, or from a different camera [25]. More generally, devising similar, domain-specific strategies to collect, verify, and measure robustness to natural perturbations in domains such as natural language processing or speech recognition is a promising direction for future work.

Acknowledgements

References

[1] Aharon Azulay and Yair Weiss. Why do deep convolutional networks generalize so poorly to small image transformations? *arXiv preprint arXiv:1805.12177*, 2018.

[2] Luca Bertinetto, Jack Valmadre, Joao F Henriques, Andrea Vedaldi, and Philip HS Torr. Fully-convolutional siamese networks for object tracking. In *European conference on computer vision*, pages 850–865. Springer, 2016.

[3] Battista Biggio and Fabio Roli. Wild patterns: Ten years after the rise of adversarial machine learning. *Pattern Recognition*, 2018. `https://arxiv.org/abs/1712.03141`.

[4] Remi Cadene. Pretrained models for pytorch. `https://github.com/Cadene/pretrain ed-models.pytorch`. Accessed: 2019-05-20.

[5] Jifeng Dai, Yi Li, Kaiming He, and Jian Sun. R-fcn: Object detection via region-based fully convolutional networks. In *Advances in neural information processing systems*, pages 379–387, 2016.

[6] Logan Engstrom, Brandon Tran, Dimitris Tsipras, Ludwig Schmidt, and Aleksander Madry. A rotation and a translation suffice: Fooling cnns with simple transformations. *arXiv preprint arXiv:1712.02779*, 2017.

[7] Alhussein Fawzi and Pascal Frossard. Manitest: Are classifiers really invariant? In *British Machine Vision Conference (BMVC)*, 2015.

[8] Christoph Feichtenhofer, Axel Pinz, and Andrew Zisserman. Detect to track and track to detect. In *Proceedings of the IEEE International Conference on Computer Vision*, pages 3038–3046, 2017.

[9] Robert Geirhos, Patricia Rubisch, Claudio Michaelis, Matthias Bethge, Felix A Wichmann, and Wieland Brendel. Imagenet-trained cnns are biased towards texture; increasing shape bias improves accuracy and robustness. *arXiv preprint arXiv:1811.12231*, 2018.

[10] Robert Geirhos, Carlos RM Temme, Jonas Rauber, Heiko H Schütt, Matthias Bethge, and Felix A Wichmann. Generalisation in humans and deep neural networks. In *Advances in Neural Information Processing Systems*, pages 7538–7550, 2018.

[11] Ian J Goodfellow, Jonathon Shlens, and Christian Szegedy. Explaining and harnessing adversarial examples. *arXiv preprint arXiv:1412.6572*, 2014.

[12] Keren Gu, Brandon Yang, Jiquan Ngiam, Quoc Le, and Jonathan Shlens. Using videos to evaluate image model robustness. *arXiv preprint arXiv:1904.10076*, 2019.

[13] Wei Han, Pooya Khorrami, Tom Le Paine, Prajit Ramachandran, Mohammad Babaeizadeh, Honghui Shi, Jianan Li, Shuicheng Yan, and Thomas S Huang. Seq-nms for video object detection. *arXiv preprint arXiv:1602.08465*, 2016.

[14] Dan Hendrycks and Thomas Dietterich. Benchmarking neural network robustness to common corruptions and perturbations. *arXiv preprint arXiv:1903.12261*, 2019.

[15] Hossein Hosseini and Radha Poovendran. Semantic adversarial examples. In *Proceedings of the IEEE Conference on Computer Vision and Pattern Recognition Workshops*, pages 1614–1619, 2018.

[16] SouYoung Jin, Aruni RoyChowdhury, Huaizu Jiang, Ashish Singh, Aditya Prasad, Deep Chakraborty, and Erik Learned-Miller. Unsupervised hard example mining from videos for improved object detection. In *ECCV*, 2018.

[17] Can Kanbak, Seyed-Mohsen Moosavi-Dezfooli, and Pascal Frossard. Geometric robustness of deep networks: analysis and improvement. *arXiv preprint arXiv:1711.09115*, 2017.

[18] Kai Kang, Hongsheng Li, Tong Xiao, Wanli Ouyang, Junjie Yan, Xihui Liu, and Xiaogang Wang. Object detection in videos with tubelet proposal networks. In *Proceedings of the IEEE Conference on Computer Vision and Pattern Recognition*, pages 727–735, 2017.

[19] Tsung-Yi Lin, Michael Maire, Serge Belongie, James Hays, Pietro Perona, Deva Ramanan, Piotr Dollár, and C Lawrence Zitnick. MS COCO detection evaluation. `http://cocodataset.org/#detection-eval`. Accessed: 2019-05-16.

[20] Tsung-Yi Lin, Michael Maire, Serge Belongie, James Hays, Pietro Perona, Deva Ramanan, Piotr Dollár, and C Lawrence Zitnick. Microsoft coco: Common objects in context. In *European conference on computer vision*, pages 740–755. Springer, 2014.

[21] Francisco Massa and Ross Girshick. maskrcnn-benchmark: Fast, modular reference implementation of Instance Segmentation and Object Detection algorithms in PyTorch. `https://github.com/facebookresearch/maskrcnn-benchmark`, 2018. Accessed: 2019-05-20.

[22] George A Miller. Wordnet: a lexical database for english. *Communications of the ACM*, 38(11): 39–41, 1995.

[23] Harold Pashler. Familiarity and visual change detection. *Perception & psychophysics*, 44(4): 369–378, 1988.

[24] Esteban Real, Jonathon Shlens, Stefano Mazzocchi, Xin Pan, and Vincent Vanhoucke. Youtube-boundingboxes: A large high-precision human-annotated data set for object detection in video. In *Proceedings of the IEEE Conference on Computer Vision and Pattern Recognition*, pages 5296–5305, 2017.

[25] Benjamin Recht, Rebecca Roelofs, Ludwig Schmidt, and Vaishaal Shankar. Do imagenet classifiers generalize to imagenet? *arXiv preprint arXiv:1902.10811*, 2019.

[26] Shaoqing Ren, Kaiming He, Ross Girshick, and Jian Sun. Faster r-cnn: Towards real-time object detection with region proposal networks. In *Advances in neural information processing systems*, pages 91–99, 2015.

[27] Olga Russakovsky, Jia Deng, Hao Su, Jonathan Krause, Sanjeev Satheesh, Sean Ma, Zhiheng Huang, Andrej Karpathy, Aditya Khosla, Michael Bernstein, Alexander C. Berg, and Li Fei-Fei. ImageNet Large Scale Visual Recognition Challenge. *IJCV*, 115(3):211–252, 2015. doi: 10.1007/s11263-015-0816-y.

[28] Antonio Torralba, Alexei A Efros, et al. Unbiased look at dataset bias. In *CVPR*, volume 1, page 7. Citeseer, 2011.

[29] Fanyi Xiao and Yong Jae Lee. Video object detection with an aligned spatial-temporal memory. In *Proceedings of the European Conference on Computer Vision (ECCV)*, pages 485–501, 2018.

[30] Cihang Xie, Yuxin Wu, Laurens van der Maaten, Alan Yuille, and Kaiming He. Feature denoising for improving adversarial robustness. *arXiv preprint arXiv:1812.03411*, 2018.

[31] Stephan Zheng, Yang Song, Thomas Leung, and Ian Goodfellow. Improving the robustness of deep neural networks via stability training. *2016 IEEE Conference on Computer Vision and Pattern Recognition (CVPR)*, Jun 2016. doi: 10.1109/cvpr.2016.485. URL `http://dx.doi.org/10.1109/cvpr.2016.485`.

[32] Xizhou Zhu, Yujie Wang, Jifeng Dai, Lu Yuan, and Yichen Wei. Flow-guided feature aggregation for video object detection. In *Proceedings of the IEEE International Conference on Computer Vision*, pages 408–417, 2017.

A   Source Dataset Overview

A.1   ImageNet-Vid

The 2015 ImageNet-Vid dataset is widely used for training video object detectors [13] as well as trackers [2]. We chose to work with the 2017 ImageNet-Vid dataset because it is a superset of the 2015 dataset. In total, the 2017 ImageNet-Vid dataset consists of 1,181,113 training frames from 4,000 videos and 512,360 validation frames from 1,314 videos. The videos have frame rates ranging from 9 to 59 frames per second (fps), with a median fps of 29. The videos range from 0.44 to 96 seconds in duration with a median duration of 12 seconds. Each frame is annotated with labels indicating the presence or absence of 30 object classes and corresponding bounding boxes for any label present in the frame. The 30 classes are ancestors of 293 of the 1,000 ILSVRC-2012 classes.

A.2   Youtube-BB

The 2017 Youtube-BB is a a large scale dataset with 8,146,143 annotated training frames 253,569 unique videos and with 1,013,246 validation frames from 31,829 videos. The video segments are approximately 19 seconds long on average. Each frame is annotated with exactly one label indicating the presence of 22 object classes, all of which are ancestors of 229 out of the ILSVRC-2012 classes.

B   Full Original vs Perturbed Accuracies

B.1   `ImageNet-Vid-Robust`

Model	Accuracy Original	Accuracy Perturbed	Δ
resnet152_finetuned	84.8 [82.5, 86.8]	70.2 [67.4, 72.8]	14.6
resnet50_finetuned	80.8 [78.3, 83.1]	65.7 [62.9, 68.5]	15.1
vgg16bn_finetuned	78.0 [75.4, 80.4]	61.0 [58.1, 63.9]	17.0
nasnetalarge_imagenet_pretrained	77.6 [75.1, 80.1]	62.1 [59.2, 65.0]	15.5
resnet50_detection	77.6 [75.1, 80.1]	65.0 [62.1, 67.8]	12.6
inceptionresnetv2_imagenet_pretrained	75.7 [73.1, 78.2]	58.7 [55.7, 61.6]	17.0
dpn107_imagenet_pretrained	75.6 [72.9, 78.1]	59.1 [56.1, 62.0]	16.5
inceptionv4_imagenet_pretrained	75.3 [72.6, 77.8]	59.0 [56.0, 61.9]	16.3
dpn92_imagenet_pretrained	74.4 [71.7, 76.9]	56.8 [53.8, 59.7]	17.6
dpn131_imagenet_pretrained	74.0 [71.3, 76.6]	59.9 [56.9, 62.8]	14.1
dpn68b_imagenet_pretrained	73.7 [71.0, 76.2]	54.0 [51.0, 57.0]	19.7
resnext101_32x4d_imagenet_pretrained	73.3 [70.6, 75.9]	57.2 [54.2, 60.1]	16.1
resnext101_64x4d_imagenet_pretrained	72.9 [70.1, 75.5]	56.6 [53.7, 59.6]	16.3
resnet152_imagenet_pretrained	72.8 [70.0, 75.4]	57.0 [54.0, 59.9]	15.8
resnet101_imagenet_pretrained	71.5 [68.7, 74.1]	53.7 [50.8, 56.7]	17.8
fbresnet152_imagenet_pretrained	71.5 [68.7, 74.1]	54.5 [51.5, 57.4]	17.0
densenet161_imagenet_pretrained	71.4 [68.7, 74.1]	55.1 [52.1, 58.1]	16.3
densenet169_imagenet_pretrained	70.2 [67.5, 72.9]	53.1 [50.1, 56.1]	17.1
densenet201_imagenet_pretrained	70.2 [67.5, 72.9]	53.4 [50.4, 56.4]	16.8

dpn68_imagenet_pretrained	69.4 [66.6, 72.1]	53.3 [50.3, 56.3]	16.1
bninception_imagenet_pretrained	69.0 [66.2, 71.7]	49.0 [46.0, 51.9]	20.0
densenet121_imagenet_pretrained	69.0 [66.2, 71.7]	50.9 [47.9, 53.8]	18.1
nasnetamobile_imagenet_pretrained	68.8 [66.0, 71.5]	48.4 [45.4, 51.4]	20.4
resnet50_augment___jpeg_compression	68.8 [66.0, 71.5]	53.2 [50.2, 56.2]	15.6
resnet34_imagenet_pretrained	68.0 [65.2, 70.7]	48.0 [45.0, 51.0]	20.0
resnet50_augment___impulse_noise	67.7 [64.9, 70.5]	50.2 [47.2, 53.2]	17.5
resnet50_augment__gaussian_blur	67.7 [64.9, 70.5]	52.5 [49.5, 55.5]	15.2
resnet50_imagenet_pretrained	67.5 [64.7, 70.3]	52.5 [49.5, 55.5]	15.0
resnet50_augment___gaussian_noise	67.4 [64.5, 70.1]	50.6 [47.6, 53.6]	16.8
resnet50_augment___shot_noise	66.5 [63.6, 69.2]	51.1 [48.1, 54.1]	15.4
vgg16_bn_imagenet_pretrained	66.4 [63.5, 69.1]	47.4 [44.5, 50.4]	19.0
resnet50_augment___defocus_blur	66.3 [63.4, 69.1]	47.6 [44.6, 50.6]	18.7
vgg19_bn_imagenet_pretrained	65.6 [62.7, 68.4]	46.6 [43.6, 49.6]	19.0
vgg19_imagenet_pretrained	63.2 [60.3, 66.1]	45.4 [42.4, 48.3]	17.8
resnet18_imagenet_pretrained	61.9 [59.0, 64.8]	41.5 [38.6, 44.4]	20.4
vgg13_bn_imagenet_pretrained	61.9 [59.0, 64.8]	43.3 [40.3, 46.3]	18.6
vgg16_imagenet_pretrained	61.4 [58.5, 64.3]	43.1 [40.2, 46.1]	18.3
vgg11_bn_imagenet_pretrained	60.9 [57.9, 63.8]	43.2 [40.3, 46.2]	17.7
vgg13_imagenet_pretrained	59.6 [56.6, 62.5]	41.1 [38.2, 44.1]	18.5
vgg11_imagenet_pretrained	57.3 [54.4, 60.3]	41.3 [38.4, 44.3]	16.0
alexnet_finetuned	57.3 [54.3, 60.2]	43.6 [40.7, 46.6]	13.7
ResNeXtDenoiseAll-101_robust_pgd	54.3 [51.3, 57.2]	40.8 [37.8, 43.7]	13.5
squeezenet1_1_imagenet_pretrained	49.8 [46.8, 52.8]	31.7 [28.9, 34.5]	18.1
alexnet_imagenet_pretrained	49.4 [46.4, 52.4]	32.0 [29.3, 34.8]	17.4
resnet50_augment___contrast_change	38.3 [35.5, 41.3]	23.3 [20.8, 25.9]	15.0

Table 5: Classification model perturbed and original accuracies for all models in our test bed evaluated on the ImageNet-Vid-Robust dataset.

B.2 **YTBB-Robust**

Model	Accuracy Original	Accuracy Perturbed	Δ
resnet152_finetuned	92.9 [91.2, 94.3]	84.7 [82.4, 86.8]	8.2
resnet50_finetuned	91.4 [89.6, 93.0]	82.0 [79.6, 84.2]	9.4
inceptionresnetv2_finetuned	91.3 [89.5, 92.9]	79.0 [76.4, 81.3]	12.3
vgg19_finetuned	90.5 [88.6, 92.2]	79.1 [76.5, 81.4]	11.4
vgg16_finetuned	89.1 [87.1, 90.8]	78.0 [75.4, 80.4]	11.1
inceptionv4_finetuned	88.5 [86.5, 90.3]	76.3 [73.6, 78.7]	12.2
resnet18_finetuned	88.0 [85.9, 89.8]	76.2 [73.6, 78.7]	11.8
alexnet_finetuned	80.6 [78.2, 82.9]	64.4 [61.5, 67.3]	16.2
pnasnet5large_imagenet_pretrained	65.2 [62.3, 68.0]	51.0 [48.0, 54.0]	14.2
nasnetalarge_imagenet_pretrained	64.9 [62.0, 67.7]	51.4 [48.4, 54.4]	13.5
inceptionresnetv2_imagenet_pretrained	64.5 [61.6, 67.4]	50.4 [47.5, 53.4]	14.1

dpn98_imagenet_pretrained	64.1 [61.2, 66.9]	49.0 [46.0, 52.0]	15.1
dpn107_imagenet_pretrained	64.1 [61.2, 66.9]	50.1 [47.2, 53.1]	14.0
dpn131_imagenet_pretrained	64.0 [61.1, 66.8]	49.9 [46.9, 52.9]	14.1
inceptionv4_imagenet_pretrained	63.6 [60.7, 66.4]	48.8 [45.8, 51.8]	14.8
xception_imagenet_pretrained	63.2 [60.2, 66.0]	47.6 [44.6, 50.6]	15.6
dpn92_imagenet_pretrained	62.3 [59.3, 65.1]	47.7 [44.8, 50.7]	14.6
resnet50_augment__jpeg_compressioon	62.3 [59.4, 65.2]	45.7 [42.8, 48.7]	16.6
polynet_imagenet_pretrained	61.4 [58.4, 64.3]	47.3 [44.4, 50.3]	14.1
nasnetamobile_imagenet_pretrained	61.4 [58.4, 64.3]	43.0 [40.1, 46.0]	18.4
resnet50_augment__shot_noise	61.3 [58.3, 64.2]	46.4 [43.4, 49.3]	14.9
dpn68_imagenet_pretrained	61.2 [58.3, 64.1]	44.2 [41.2, 47.2]	17.0
fbresnet152_imagenet_pretrained	61.1 [58.1, 64.0]	45.9 [42.9, 48.8]	15.2
resnet152_imagenet_pretrained	60.8 [57.8, 63.7]	46.5 [43.5, 49.5]	14.3
resnet101_imagenet_pretrained	60.8 [57.8, 63.7]	45.2 [42.2, 48.2]	15.6
senet154_imagenet_pretrained	60.7 [57.7, 63.6]	47.2 [44.3, 50.2]	13.5
resnet50_augment__impulse_noise	60.6 [57.7, 63.5]	45.5 [42.6, 48.5]	15.1
se_resnet101_imagenet_pretrained	60.5 [57.6, 63.4]	45.6 [42.6, 48.6]	14.9
bninception_imagenet_pretrained	60.4 [57.4, 63.3]	41.8 [38.9, 44.7]	18.6
densenet161_imagenet_pretrained	60.2 [57.3, 63.1]	46.4 [43.4, 49.4]	13.8
resnet50_augment__gaussian_noise	60.2 [57.3, 63.1]	45.7 [42.8, 48.7]	14.5
se_resnext50_32x4d_imagenet_pretrained	59.9 [56.9, 62.8]	45.7 [42.7, 48.6]	14.2
dpn68b_imagenet_pretrained	59.7 [56.7, 62.6]	45.9 [42.9, 48.8]	13.8
inceptionv3_imagenet_pretrained	59.6 [56.6, 62.5]	43.8 [40.8, 46.8]	15.8
densenet121_imagenet_pretrained	59.5 [56.5, 62.4]	43.1 [40.1, 46.0]	16.4
se_resnext101_32x4d_imagenet_pretrained	59.2 [56.3, 62.1]	45.2 [42.3, 48.2]	14.0
densenet201_imagenet_pretrained	59.2 [56.2, 62.1]	44.8 [41.8, 47.8]	14.4
densenet169_imagenet_pretrained	59.2 [56.2, 62.1]	44.6 [41.7, 47.6]	14.6
resnet50_augment__brightness_change	58.9 [56.0, 61.8]	42.6 [39.6, 45.5]	16.3
se_resnet50_imagenet_pretrained	58.8 [55.9, 61.7]	44.1 [41.1, 47.1]	14.7
se_resnet152_imagenet_pretrained	58.8 [55.9, 61.7]	44.8 [41.9, 47.8]	14.0
cafferesnet101_imagenet_pretrained	58.2 [55.2, 61.1]	44.3 [41.3, 47.3]	13.9
resnet50_augment__regular	58.0 [55.1, 61.0]	42.9 [39.9, 45.8]	15.1
resnet34_imagenet_pretrained	57.9 [55.0, 60.9]	42.8 [39.8, 45.7]	15.1
vgg19_imagenet_pretrained	57.5 [54.6, 60.5]	40.1 [37.2, 43.1]	17.4
resnet50_augment__gaussian_blur	57.5 [54.5, 60.4]	41.8 [38.9, 44.7]	15.7
vgg16_bn_imagenet_pretrained	57.2 [54.2, 60.1]	39.6 [36.7, 42.6]	17.6
resnet50_imagenet_pretrained	57.0 [54.1, 60.0]	43.8 [40.9, 46.8]	13.2
vgg19_bn_imagenet_pretrained	56.8 [53.9, 59.8]	40.6 [37.7, 43.5]	16.2
vgg16_imagenet_pretrained	55.4 [52.4, 58.4]	40.1 [37.2, 43.1]	15.3
vgg13_bn_imagenet_pretrained	54.8 [51.8, 57.7]	38.6 [35.7, 41.6]	16.2
vgg11_bn_imagenet_pretrained	54.8 [51.8, 57.7]	38.8 [35.9, 41.8]	16.0
vgg11_imagenet_pretrained	54.7 [51.7, 57.6]	38.4 [35.5, 41.3]	16.3
resnet18_imagenet_pretrained	54.4 [51.4, 57.4]	38.1 [35.2, 41.0]	16.3
vgg13_imagenet_pretrained	54.2 [51.3, 57.2]	37.7 [34.9, 40.7]	16.5
ResNeXtDenoiseAll-101_robust_pgd	53.6 [50.7, 56.6]	43.2 [40.2, 46.1]	10.4

squeezenet1_0_imagenet_pretrained	**51.1** [48.1, 54.1]	**33.1** [30.3, 36.0]	18.0
squeezenet1_1_imagenet_pretrained	**48.6** [45.6, 51.6]	**31.3** [28.6, 34.2]	17.3
resnet50_augment__defocus_blur	**48.4** [45.4, 51.4]	**29.1** [26.4, 31.8]	19.3
alexnet_imagenet_pretrained	**45.3** [42.4, 48.3]	**30.5** [27.8, 33.3]	14.8

Table 6: Classification model perturbed and original accuracies for all models in our test bed evaluated on the YTBB-robust dataset..

C   Model independent distribution shift

Though the distribution shift we induced in our study were *model dependent* because we found the worst neighbor frame *for each* model, we could study the same problem but impose a static set of perturbed frames across all models. In Figure 6 we study this static set of perturbations across all models and see a substantial (but smaller) drop in accuracy for both models. The static set of perturbations were chosen by choosing the neighbor frame that the largest number of models got incorrectly.
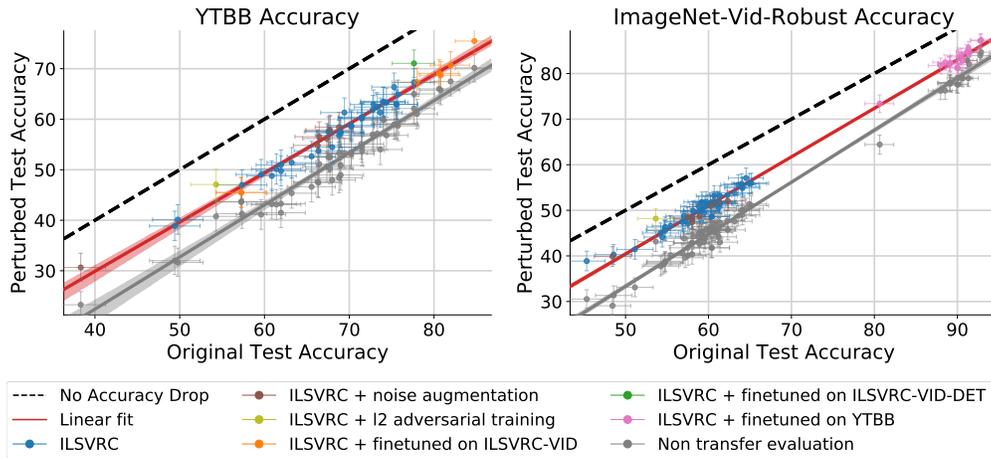

Figure 6: Model accuracy on original vs. perturbed images for a static set of perturbed frames across all models. The grey points and grey linear fit correspond to the perturbed accuracies of models evaluated on per model perturbations studied in Figure 3

D   Per class analysis

We study the effect of our perturbations on the 30 classes in `ImageNet-Vid-Robust` and `YTBB-Robust` to determine whether the performance drop was concentrated in a few "hard" classes. Figure 7 shows the original and perturbed accuracies across classes for our best performing model (a fine-tuned ResNet-152). Although there are a few particularly difficult classes for perturbed accuracy (e.g., lion or monkey on `ImageNet-Vid-Robust`), the accuracy drop is spread across most classes. On `ImageNet-Vid-Robust`, this model saw a total drop of 14.4% between original and perturbed images and a median drop of 14.0% in per-class accuracy. On `YTBB-Robust`, the total drop was 8.9% and the median drop was 6.7%.
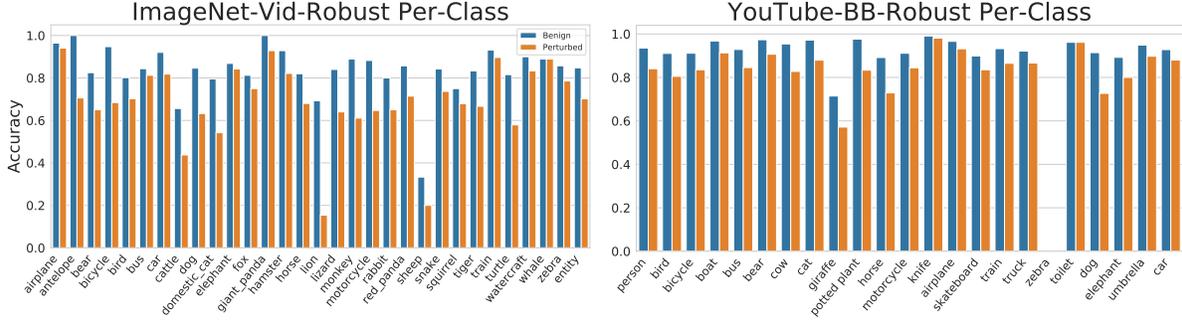
Figure 7: Per-class accuracy statistics for our best performing classification model (fine-tuned ResNet152) on `ImageNet-Vid-Robust` and `YTBB-Robust`. For Youtube-BB, note that 'zebra' is the least common label, present in only 24 anchor frames sampled by [12], of which 4 are included in our dataset.

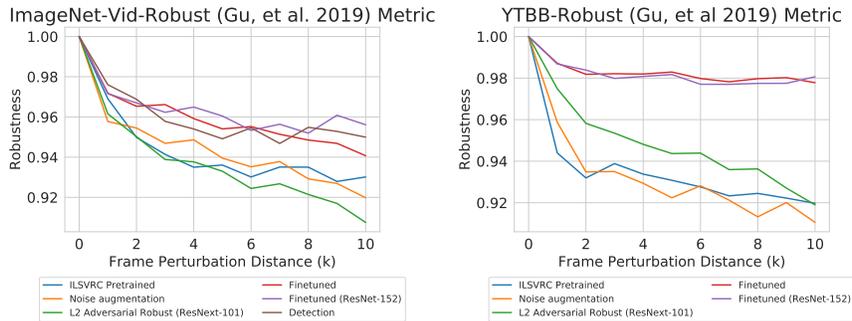# E   Per-frame conditional robustness metric introduced in [12]

Figure 8: Conditional robustness metric from [12] on perturbed frames as a function of perturbation distance on `ImageNet-Vid-Robust` and `YTBB-Robust`. Model accuracies from five different model types and the best performing model are shown. The model architecture is ResNet-50 unless otherwise mentioned.

In concurrent work, the authors of [12] considered a different metric of robustness. In this section, we compute this metric on all models in our test bed to compare our findings to [12]. There are two main differences between PM-k and the robustness metric in [12].

1. For two visually similar "neighbor" frames I_0 and I_1 with true label Y and classifier f, [12] studies the conditional probability $P(f(I_1) = y | f(I_0) = y)$

2. While PM-k looks for errors in all neighbor frames in a neighborhood of k frames away from the anchor frame (so this would include frames 1, 2, ..., k frames away), [12] only considers errors from **exactly** k frames away.

In Fig. 9 we illustrate simple example where two videos can have the same behavior for the metric introduced by [12] but drastically different behavior for the PM-kmetric.
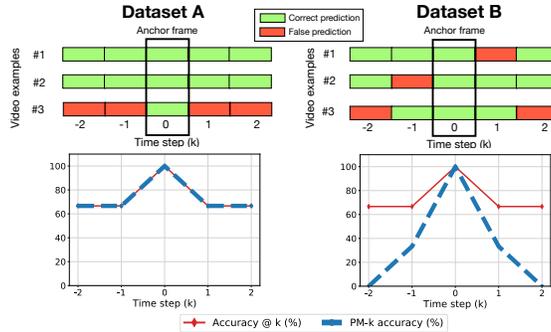
Figure 9: For the two example videos above the score from [12] metric (Accuracy @ K) is identical, but the PM-k metric behaves substantially differently when the errors are spread across many independent videos, as shown in the right example

F ℓ_∞ distance vs PM-k Accuracy

ℓ_∞ adversarial examples are well studied in the robustness community, yet the connection between ℓ_∞ and other forms of more "natural" robustness is unclear. Here, we plot the cumulative distribution of the ℓ_∞ distance between pairs of nearby frames in our datasets. In Figure 10, we show the CDF of ℓ_∞ distance for all pairs, all reviewed pairs, and mistakes made by 3 indicative models. Note the `fbrobust` model is trained specifically to be robust to ℓ_∞ adversaries.
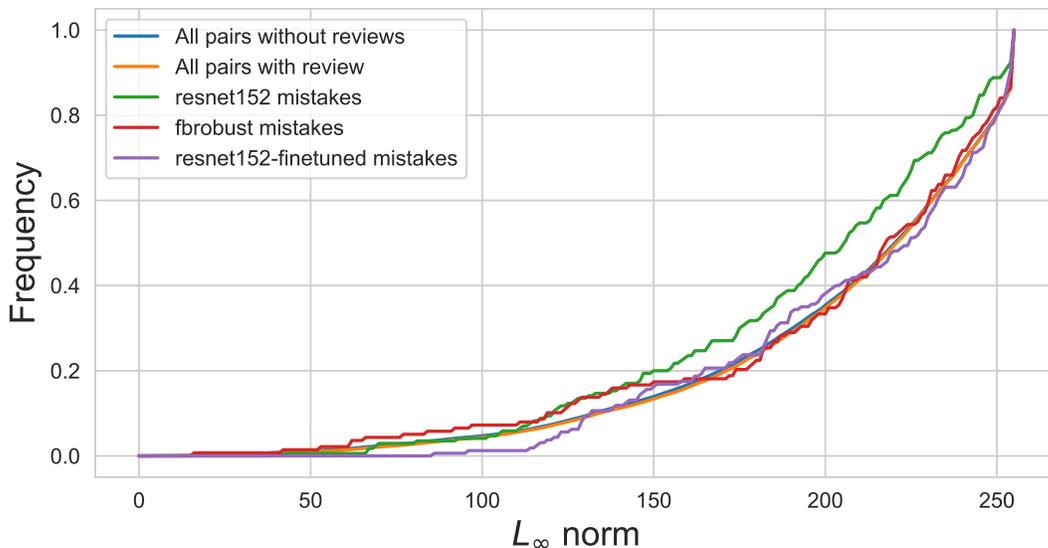

Figure 10: CDF showing the ℓ_∞ distance between pairs of frames from different distributions.

G PM-k Accuracy with varying k
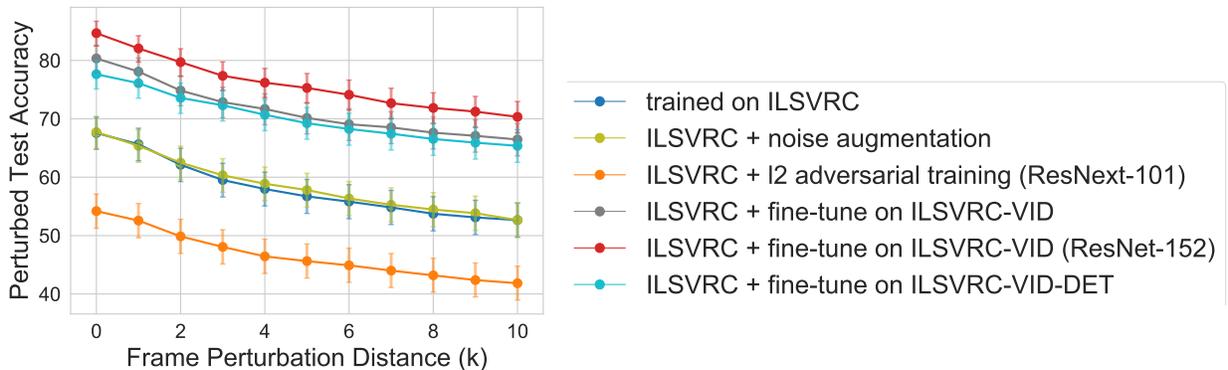
G.1 **ImageNet–Vid–Robust**

Figure 11: Model classification accuracy on perturbed frames as a function of perturbation distance (shown with 95% Clopper-Pearson confidence intervals). Model accuracies from five different model types and the best performing model are shown. The model architecture is ResNet-50 unless otherwise mentioned.

In Figure 11, we plot the relationship between acc_{pmk} and perturbation distance (i.e., the k in the pm-k metric). The entire x-axis in Figure 11 corresponds to a temporal distance of at most 0.3 seconds between the original and perturbed frames.

H I-frames and P-Frames

H.1 **ImageNet–Vid–Robust**

One possible concern with analyzing performance on video frames is the impact of video compression on model robustness. In particular, the videos in ImageNet-Vid-Robust contain 3 different frame types: 'i-frames', 'p-frames', and 'b-frames'. 'p-frames' are compressed by referencing pixel content from previous frames, while 'b-frames' are compressed via references to previous and future frames. 'i-frames' are stored without references to other frames.

We compute the original and perturbed accuracies, and the drop in accuracy for a subset of the dataset without 'i-frames', a subset without 'p-frames', and a subset without 'b-frames' in Table 7. While there are modest differences in accuracy due to compression, this analysis suggests that the sensitivity of models is not significantly due to the differences in quality of frames due to video compression.

Table 7: Analyzing results based on frame-type in video compression. See Appendix H.1 for details.

	Original Acc.	Perturbed Acc.	Δ	# anchor frames
All frames	84.8	70.2	14.6	1109
w/o 'i-frames'	84.7	70.3	14.4	1104
w/o 'p-frames'	83.9	73.7	10.2	415
w/o 'b-frames'	85.4	73.2	12.2	699

I FPS analysis

I.1 `ImageNet-Vid-Robust`

To analyze the impact of frame-rate on accuracy, we show results on subsets of videos with fixed fps (25, 29, and 30, which cover 89% of the dataset) using a fine-tuned ResNet-152 model in Table 8. The accuracy drop is similar across the subsets, and similar to the drop for the whole dataset.

FPS	Acc. Orig.	Acc. Perturbed	Drop	# Videos
25	87.3 [83.0, 90.9]	73.3 [67.8, 78.3]	14.0	292
29	87.7 [84.0, 90.8]	74.9 [70.3, 79.2]	12.8	383
30	78.3 [73.3, 82.7]	61.7 [56.0, 67.1]	16.6	313

Table 8: Results on subsets of ImageNet-Vid-Robust with fixed FPS.

J ILSVRC training with `ImageNet-Vid-Robust` classes

We trained ResNet-50 from scratch on ILSVRC using the 30 ImageNet-Vid classes. We also fine-tuned the model on ImageNet-Vid. In Table 9, we show the accuracy drops are consistent with models in our submission. We hypothesize that the lower accuracy is due to coarser supervision on ILSVRC.

Model	Acc. Orig.	Acc. Perturbed	Drop
ILSVRC-30	61.0	44.9	15.1
ILSVRC-30 + FT	77.8	59.9	17.9

Table 9: Results of training ResNet-50 on ILSVRC with 30 classes from `ImageNet-Vid-Robust`.

K Experimental Details & Hyperparameters

All classification experiments were carried out using PyTorch version 1.0.1 on an AWS p3.2xlarge with the NVIDIA V100 GPU. All pretrained models were downloaded from [4] at commit hash `021d97897c9aa76ec759deff43d341c4fd45d7ba`. Evaluations in Tables B.1 and B.2 all use the default settings for evaluation. The hyperparameters for the *fine-tuned* models are presented in Table 10. We searched for learning rates between 10^{-3} and 10^{-5} for all models.

We additionally detail hyperparameters for detection models in Table 11. Detection experiments were conducted with PyTorch version 1.0.1 on a machine with 4 Titan X GPUs, using the Mask

R-CNN benchmark repository[21]. We used the default learning rate provided in [21]. For R-FCN, we used the model trained by [29].

Table 10: Hyperparameters for models finetuned on ImageNet-Vid,

Model	Base Learning Rate	Learning Rate Schedule	Batch Size	Epochs
resnet152	10^{-4}	Reduce LR On Plateau	32	10
resnet50	10^{-4}	Reduce LR On Plateau	32	10
alexnet	10^{-5}	Reduce LR On Plateau	32	10
vgg16	10^{-5}	Reduce LR On Plateau	32	10

Table 11: Hyperparameters for detection models.

Model	Base Learning Rate	Learning Rate Schedule	Batch Size	Iterations
F-RCNN ResNet-50	10^{-2}	Step 20k, 30k	8	40k
F-RCNN ResNet-101	10^{-2}	Step 20k, 30k	8	40k

L   Detection pm-k

We briefly introduce the mAP metric for detection here and refer the reader to [19] for further details. The standard detection metric proceeds by first determining whether each predicted bounding box in an image is a true or false positive, based on the intersection over union (IoU) of the predicted and ground truth bounding boxes. The metric then computes the per-category average precision (AP, averaged over recall thresholds) of the predictions across all images. The final metric is reported as the mean of these per-category APs (mAP).

We define the pm-k analog of mAP by replacing each anchor frame in the dataset with a nearby frame that minimizes the per-image average precision. Since the category-specific average precision is undefined for categories not present in an image, we minimize the average precision across categories present in each frame rather than the mAP.